Electrochemical Impedance Spectroscopic Study on Eu^{2+} and Sr^{2+} Using Liquid Metal Cathodes in Molten Chlorides

Masahiko Matsumiya and Ryuzo Takagi[a]

Central Research Institute of Electric Power Industry, Nuclear Fuel Cycle Department, Komae Research Laboratory, 2-11-1, Iwado Kita, Komae-shi, Tokyo 201-8511 Japan

[a] Research Laboratory for Nuclear Reactors, Tokyo Institute of Technology, O-okayama, Meguro-ku, Tokyo 152-8550 Japan.

Reprint requests to Prof. M. M.; Fax: 81 3-3480-7956, E-mail: kommatsu@criepi.denken.or.jp

Z. Naturforsch. **55 a,** 673–681 (2000); received April 25, 2000

For the pyrochemical reprocessing of spent metallic nuclear fuels in molten salt baths it is important to investigate the behavior of the electrochemically negative elements Eu and Sr, which are significant fission products. Voltammetric and chronopotentiometric studies have shown that the reduction of Eu^{2+} and Sr^{2+} on liquid Pb cathodes in molten chloride baths at 1073 K follows the alloy formation reaction: $Eu^{2+} + 2e^- + 3Pb \rightarrow EuPb_3$ and $Sr^{2+} + 2e^- + 3Pb \rightarrow SrPb_3$. In the present work these alloy formation reactions were studied by electrochemical impedance spectroscopy. Analysis of the spectra showed that the electronic exchange of Eu^{2+}/Eu and Sr^{2+}/Sr is quasi-reversible. Moreover, the experimental results allowed the determination of the kinetic parameters of Eu^{2+}/Eu and Sr^{2+}/Sr, the diffusion coefficients of these species in molten chloride baths, and also the diffusion layer thickness.

Key words: Alloy Formation Reaction; Europium; Impedance; Liquid Metal Cathodes; Molten Salts; Strontium.

1. Introduction

In nuclear energy technology one should become able to separate the fission products from one another for incineration and winning of medical tracers. Therefore we have studied the pyrochemical treatment of metallic fuel proposed by ANL [1 - 3]. After the electrorefining and drawdown process, all alkali, alkaline-earth and more electrochemically basic rare earth residues remain in the fused salt bath. Thus, fission products like alkali and alkaline-earth elements in the salt phase can be recovered by recycling the salt bath. However, it is troublesome to recover these elements from the salt bath because of their more negative decomposition potentials [4] than those of the components of the solvent. Therefore we have previously performed an electrochemical investigation of the alloy formation mechanism of the electrochemically negative elements (Eu^{2+} [5], Sr^{2+} [5], Ba^{2+} [6, 7] and Cs^+ [8]) in molten chloride and fluoride systems by means of transitory techniques (voltammetry and chronopotentiometry). The results revealed that the alloy formation reactions of Eu^{2+}, Sr^{2+} and Ba^{2+} can be qualified as quasi-reversible reactions on a liquid Pb electrode at 1073 K. In addition, for Ba^{2+} [7] we have reported that the order of the thermodynamic characteristics and activity coefficients for each cathode is consistent with the tendency of the selectivity in our results. To our knowledge there are no previously published electrochemical impedance spectroscopy (EIS) studies of the electrochemistry of Eu^{2+} and Sr^{2+} in fused NaCl-KCl and KCl systems at 1073 K. We were anxious to verify that this mechanism could be deduced by using impedance measurements. The experimental diagrams were then compared to simulated ones using the proposed equivalent circuits.

2. Experimental

(a) Melt Preparation

NaCl obtained from Wako Chem. Ind. Ltd.: > 99.5%, KCl from Kanto Chem. Ind. Ltd.: > 99.5%, $EuCl_2$ from APL Engineered Materials, Inc.: 99.99%, and $SrCl_2$ from Wako Chem. Ind. Ltd.: > 99.5%). The finely crushed alkali chlorides were mixed in the

0932–0784 / 00 / 0800–0673 $ 06.00

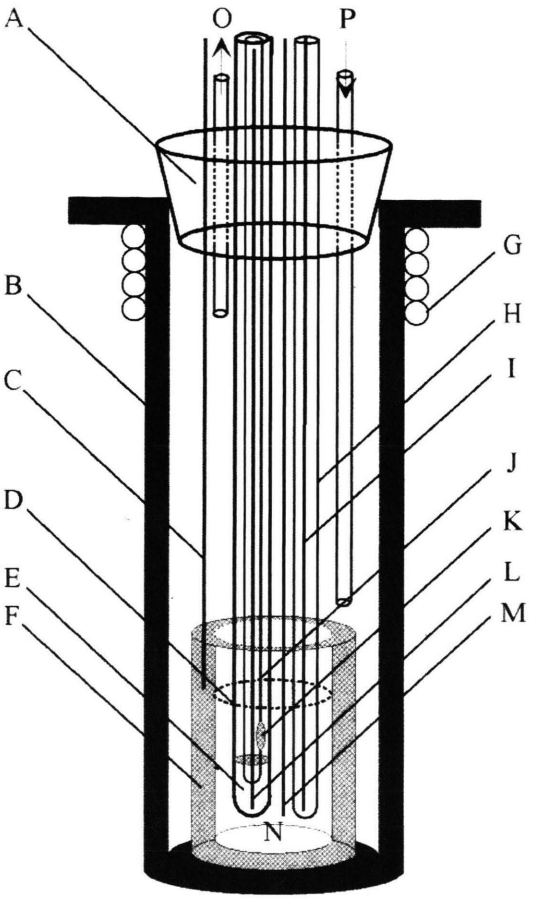

Fig. 1. Experimental cell adapted for EIS measurement in molten chloride bath at 1073 K; A: Silicon stopper, B: Stainless steel cell, C: Tungsten wire (lead to crucible), D: Quartz tube (covering the liquid electrode), E: Liquid Pb working electrode, F: Graphite crucible (counter electrode), G: Cooling water, H: Quartz tube (covering thermocouple), I: Thermocouple, J: Quartz tube (covering tungsten wire), K: 6mmø hole, L: Tungsten wire (lead to liquid Pb), M: Pt wire (quasi-reference electrode), N: Molten salts, O: Ar gas outlet, P: Ar gas inlet.

molar ration 1:1, introduced in a quartz cell, dehydrated by heating under vacuum at 973 K for about 7 h and then melted at 1073 K. The solute was also dehydrated in a quartz cell by heating under vacuum at about 673 K for about 24 h. Pb was obtained from Wako Chem. Ind. Ltd.: > 99.9%.

(b) Electrodes and Electrical Devices

The cell for the voltammetric and chronopotentiometric experiments has been described in [5]. A similar type of cell, depicted in Fig. 1, was used for the present measurement of EIS. The quasi-reference electrode was a Pt wire (1.5 mmø, Nilaco Co.: > 99.98%). Platinum does not alloy with Eu, Sr and alkali metals, exhibits a high electrochemical stability, and its practical oxidation potential is close to the value at which chlorine gas is evolved. The Pb electrode was rinsed in 1N HNO_3 and degreased with acetone before use. Before the electrochemical experiments, pre-electrolysis was carried out with a tungsten electrode under a constant current. A graphite crucible (MS-G, Tokai Carbon: > 99.9%) was used as counter electrode. A tungsten wire (1.5mmø, Nilaco Co.: > 99.98%) was connected to this crucible with a ceramic binder. The preparation of the liquid Pb electrode is described in [5]. For the EIS, a 2-channels and 2-phases rock-in amplifier and a sine-wave generator (HECS 332B: Fuso) was used with a potentio/galvanostat (Type 2001, Toho Tech.).

3. Results and Discussion

(a) Previous Transitory Techniques [5]

The voltammograms in [5] were obtained with a liquid Pb electrode in NaCl-KCl-$EuCl_2$ and KCl-$SrCl_2$ systems. The peaks, characteristic for systems with soluble oxidant and reductant, were attributed to Eu^{2+}/Eu and Sr^{2+}/Sr exchanges. The cathodic peak currents were proportional to the square root of the sweep rates. These results indicate that the arrival of the electroactive species at the surface of the electrode was kinetically controlled by the diffusion of Eu^{2+} and Sr^{2+}.

(b) Impedancemetry on the Tungsten Electrode

The linearity domain of the system in our study was verified by a comparison of the responses at different frequencies on imposing excitation signals of increasing amplitudes. In our experiments we verified that the modulus of the real part of the electrode impedance remained constant below –1.50 V (vs. Pt Q.R.E). EIS measurements were performed over a frequency range of $3 \cdot 10^4$ Hz - 10^{-2} Hz, using a perturbation signal with an amplitude of 5 or 10 mV/s. We applied the simple model modified in [9, 10] to the equivalent circuit in our measurements. The most simple model of the impedance of a working electrode in an electrolyte where a Faraday process proceeds is a parallel combination of the Faradaic impedance

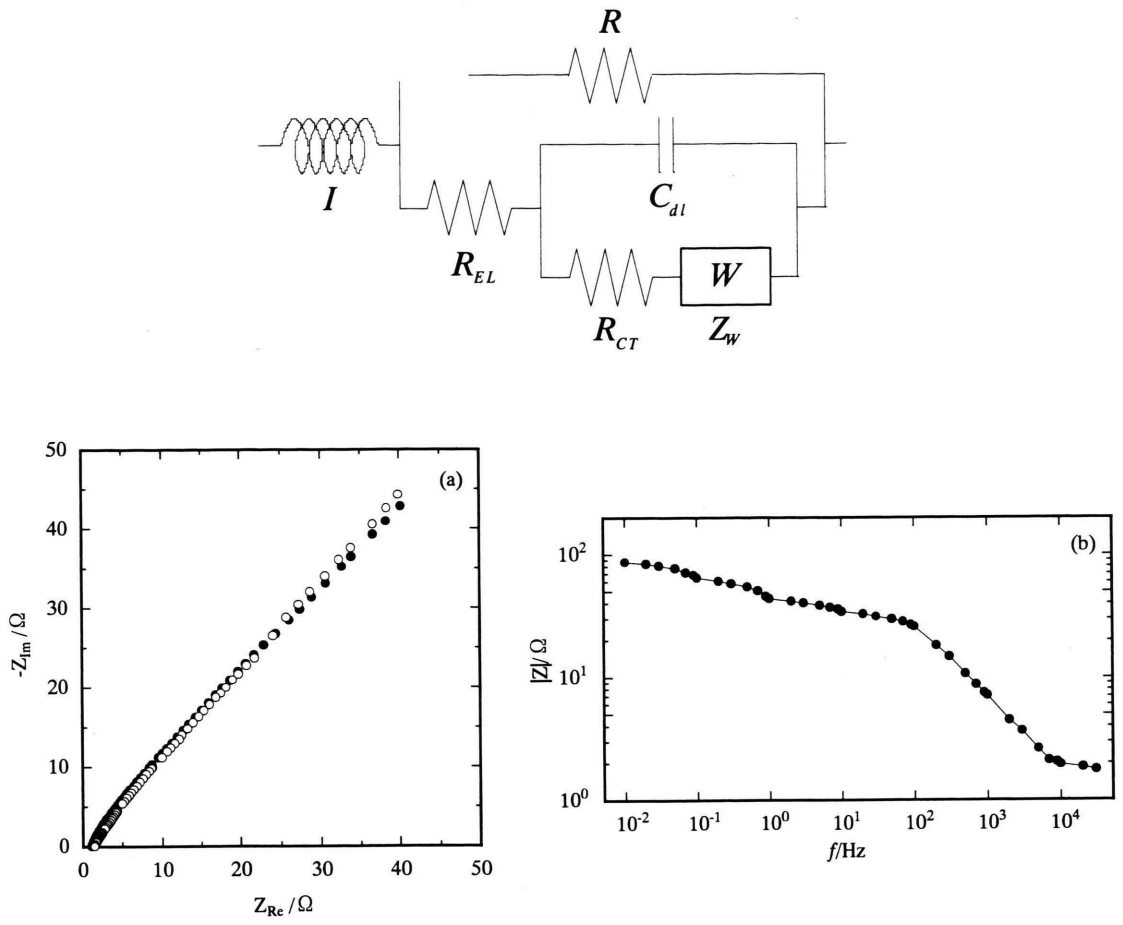

Fig. 2. Typical Impedance diagram on a tungsten electrode in molten NaCl-KCl equimolar mixtures including $SrCl_2$ at 1073K in comparison with simulated results in the case of diffusion-convection. (a) Nyquist plots measured (white circles) and calculated (black circles). (b) Bode representation, measured (black points) and calculated (solid lines), which corresponds to the equivalent circuit shown (I: inductivity; R_{EL}: ohmic resistance of electrolyte; R_{CT}: charge-transfer resistance; Z_W: Warburg impedance; C_{dl}: capacitance of the double layer; R: electronic resistance) in the frequency range 10^{-2} Hz < f < $3 \cdot 10^4$ Hz.

(the charge transfer resistance in series with the Warburg diffusion impedance) and the double layer capacitance. This parallel combination is in series with the ohmic resistance of the electrolyte which is with a parallel combination of electronic resistance. This combination is in series with an inductivity.

The stationarity of the system was ensured by control before and after each measurement of the constancy of the current and potential. The stability of the system was also verified by always recording the impedance spectra one increasing and decreasing scanning of frequencies. The superposition of the obtained diagrams allowed us to conclude that the system was stable.

Typical EIS spectra in the complex plane obtained for $SrCl_2$ in molten NaCl-KCl on a tungsten electrode are compared to simulated waves in Figure 2. The general shape of the spectrum agreed well with the one expected for a diffusion-convection controlled rapid exchange. The slope of the linear part of the diagram was near unity, which proved that this impedance could be related to the mass transport of an electroactive species. The tungsten electrode was submitted to different applied potentials. The evolutions of the electrode impedance in the complex plane for $SrCl_2$ and $EuCl_2$ in molten NaCl-KCl on a tungsten electrode are indicated in Figs. 3 (a) - (d) and 3 (e) - (h), respectively. In the applied range the diagrams have a

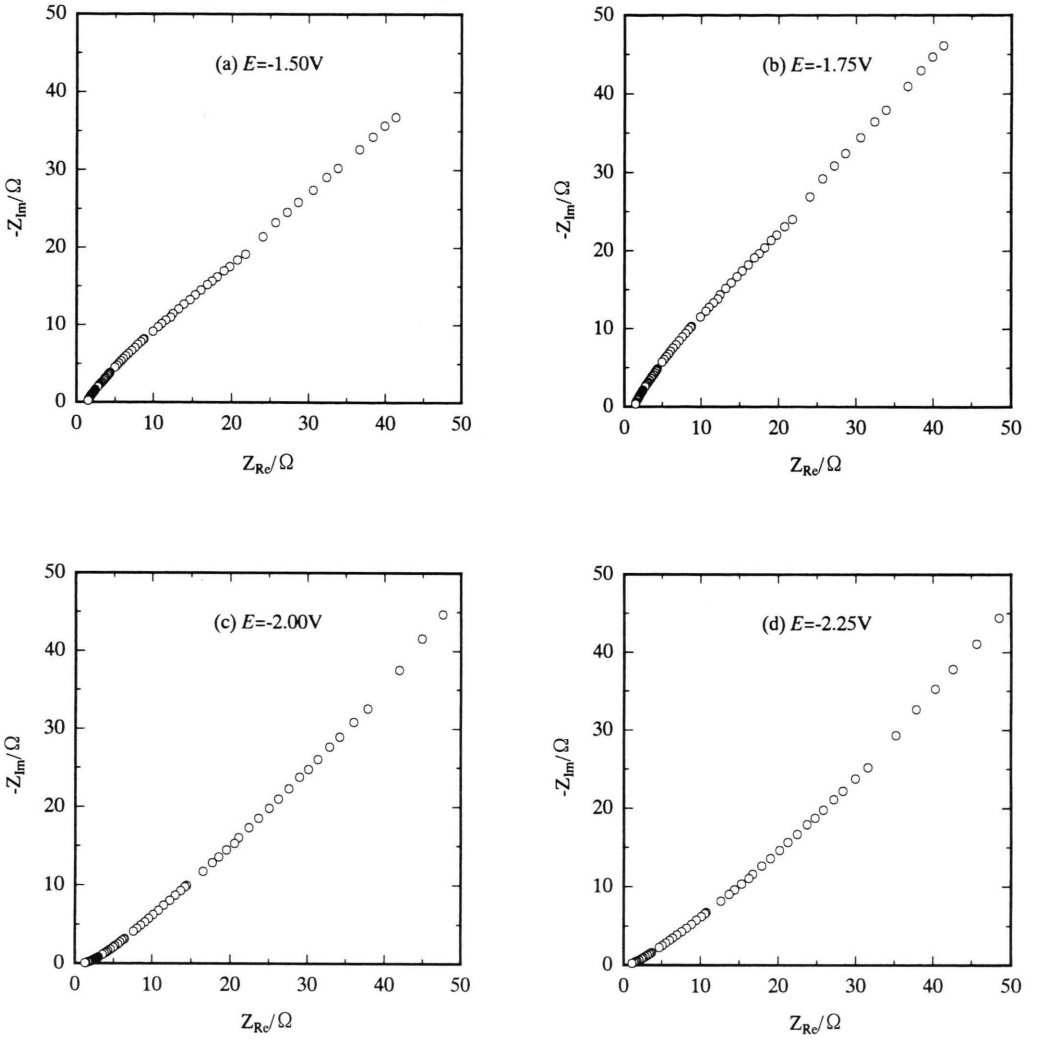

Fig. 3. Impedance diagrams of $SrCl_2$ (a) –1.50 V, (b) –1.75 V, (c) –2.00 V, (d) –2.25 V (vs. Pt Q.R.E) and $EuCl_2$ (e) –1.75 V, (f) –2.00 V, (g) –2.25 V, (h) –2.50 V (vs. Pt Q.R.E) on the tungsten electrode for different applied potential values.

diffusion-convection shape. Next, the diagrams tend to show Warburg diffusion for applied potential less than –1.50 V. The diffusion layer thickness became infinite. A charge transfer semi-circle was not observed at any potential.

(c) Impedancemetry on the Liquid Pb Electrode

A typical impedance plot obtained for $EuCl_2$ in the NaCl-KCl system on the liquid Pb electrode is presented in Fig. 4 which shows a circular arc at high frequencies, followed by a linear behavior with a slope close to 45°, indicating a mass transfer limited process at low frequencies. The data dispersion could be ascribed to movements of the liquid electrode under polarization: This feature was noticed by several authors when using liquid metal electrodes [11 - 13]. It has been reported that the current oscillations depend rather on the nature of the electrode than on it's geometry; these conclusions are applicable to a liquid metal-molten salt surface as well as to a liquid metal-aqueous solution interface [11].

The electrolyte resistance, R_{EL}, measured by current interruption was $R_{EL} = 0.38\ \Omega$ in agreement with the value read in the impedance diagrams. The experimental diagrams were simulated considering, es-

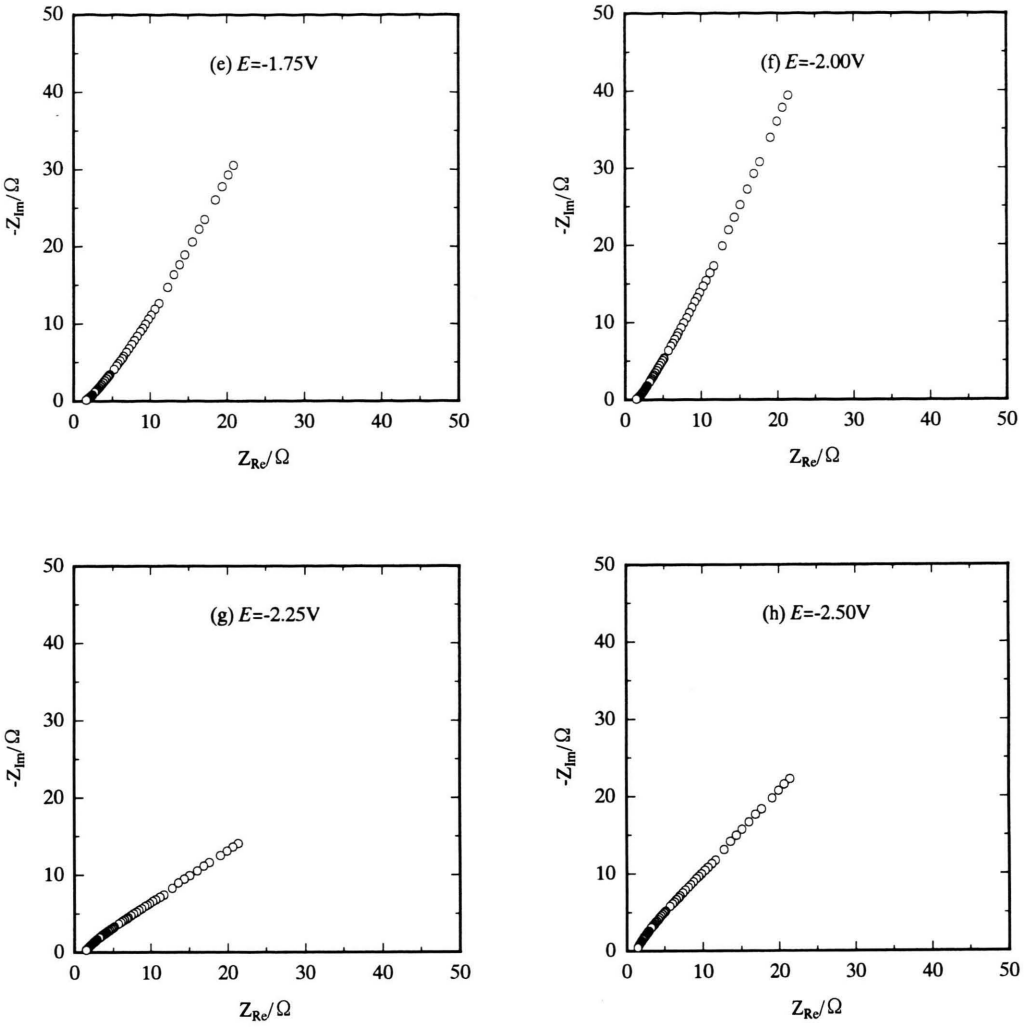

Fig. 3 (continued).

pecially at high frequencies, the improved equivalent circuits with the adsorption term, and the good agreement obtained between the experimental and calculated curves (Fig. 4) confirms that the rate determining steps occur in the reactional pathway proposed. The adsorption occurs at liquid metallic electrodes. The best fittings lead to a charge transfer resistance R_{CT} of 0.106 Ω for $EuCl_2$. This value indicates that the charge transfer is rather rapid.

The diffusion coefficient, D can be evaluated using the equation [14]

$$\sigma = \frac{RT}{\sqrt{2}n^2F^2AC^*D^{1/2}}, \tag{1}$$

where σ is the Warburg coefficient, n the charge transfer number, F the Faraday constant, A the electrode area, C^* the bulk concentration of the electroactive species, R the gas constant and T the absolute temperature. For $n = 2$ and $\sigma = 0.279\ \Omega\cdot s^{-1/2}$, determining the slope as found in Fig. 5, we found $D = 1.34\cdot10^{-5}cm^2s^{-1}$ for Eu^{2+} and $D = 1.42\cdot10^{-5}cm^2s^{-1}$ for Sr^{2+}. The diffusion coefficient of Sr^{2+} is in reasonable agreement with the value $1.46\pm0.18\cdot10^{-5}cm^2s^{-1}$ reported by Volkovich [15]. The obtained diffusion coefficient of Eu^{2+} is close to that of Sr^{2+}, probably due to the analogous behavior of the reduction mechanism for the alloy formation reaction and the similarity of the ionic radii of Eu^{2+},

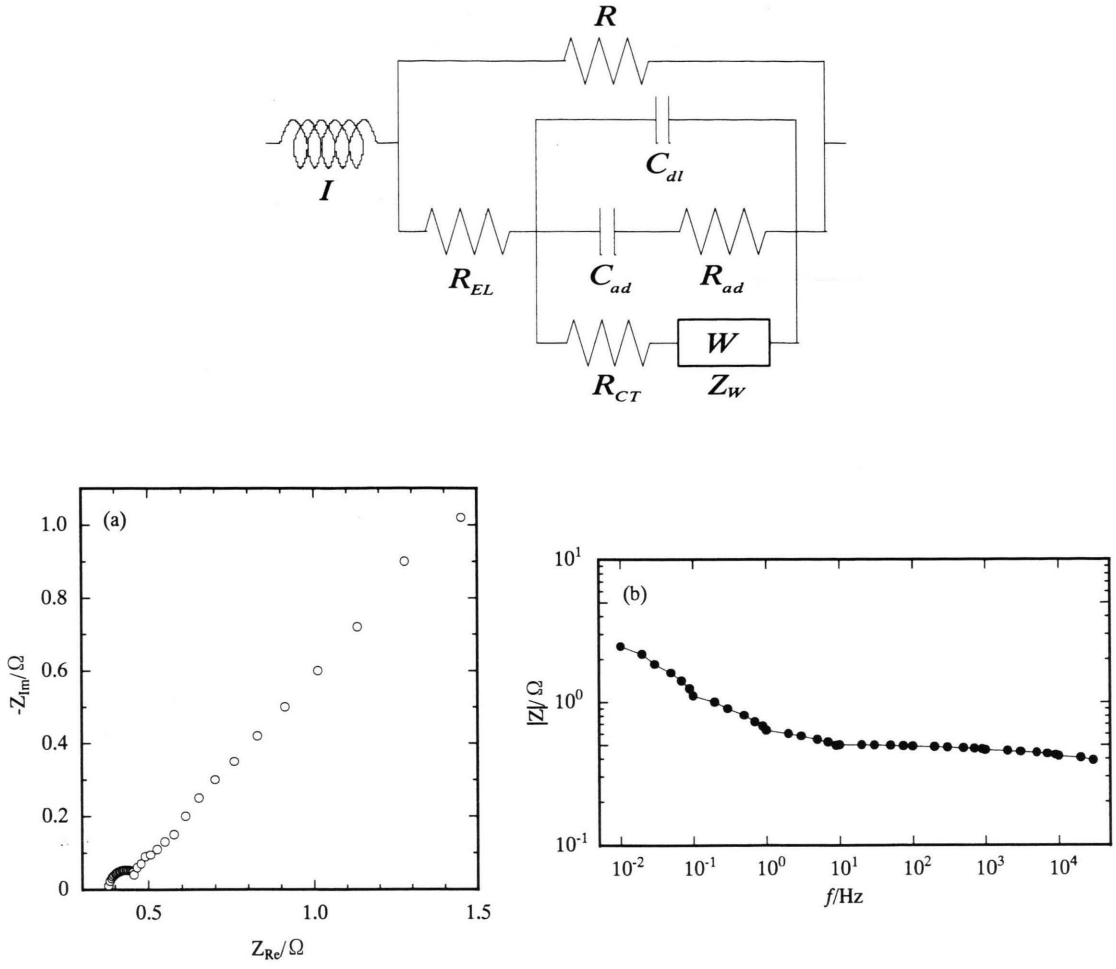

Fig. 4. Typical impedance diagram of $EuCl_2$ on a liquid Pb electrode in molten NaCl-KCl equimolar mixtures at 1073K, (a) Nyquist plots (b) Bode representation, measured (black points) and calculated (solid lines) which including an adsorption term (R_{ad} in series with C_{ad}) coupled in parallel with the Faradaic impedance and double-layer capacitance in the frequency range; 10^{-2} Hz < f < $3{\cdot}10^{4}$ Hz. Explanation of the other elements is given in the legend to Figure 2.

Sr^{2+}, and Pb^{2+}. (Eu^{2+}: 0.117 nm, Sr^{2+}: 0.118 nm, Pb^{2+}:0.119 nm [16]). It was reported that the energies of the band dissociation according to an analysis of the thermochemical data also virtually coincide for Eu and Sr [17]. This result is consistent with our experimental results.

Knowledge of the value of D enables to estimate the thickness δ of the diffusion layer from the cathodic plateau of the stationary current-potential curve, which is expressed as

$$|i| = nFAC^* \frac{D}{\delta}, \tag{2}$$

where i is the limiting (plateau) current density. We found $\delta = 5.4{\cdot}10^{-3}$ cm.

Furthermore, since the impedance measurements were obtained at the rest potential, the following expression can be used for the charge transfer resistance:

$$R_{ct} = \frac{RT}{nF}\frac{1}{i_0} = \frac{RT}{n^2F^2Ak^0C^*\alpha^2}, \tag{3}$$

where i_0 is the exchange current density, k^0 is the standard rate constant, and α the charge transfer coefficient. This expression allows the calculation of k^0 assuming $\alpha = 0.5$: $k^0 = 2.92{\cdot}10^{-2}$cm s^{-1} for Eu^{2+} and $2.43{\cdot}10^{-2}$cm s^{-1} for Sr^{2+}. Thus, the alloy formation

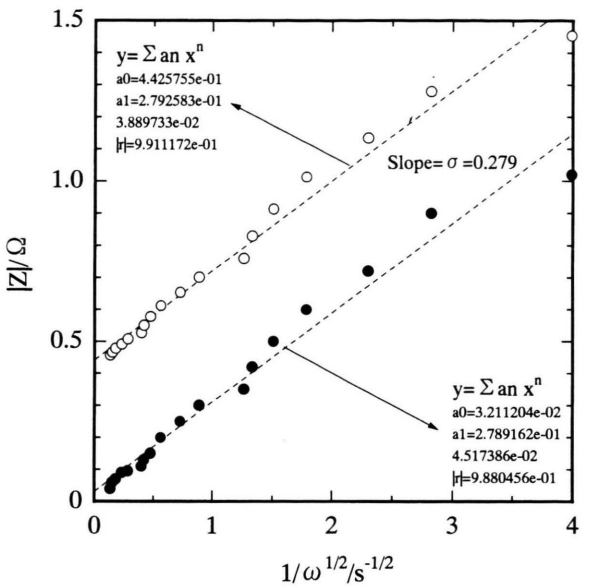

Fig. 5. Relationship between the inverse of the square root of the pulsation and the real and imaginary part of overall impedance for $EuCl_2$ in the NaCl-KCl system on the liquid Pb electrode at 1073 K in the lower frequency ranges, ○: real part, ●: imaginary part.

reactions between Eu, Sr and Pb can be qualified as quasi-reversible at 1073 K according to the Matsuda and Ayabe criterion [18]. These reduction processes, which are interrelated with the alloy formation reactions are consistent with the previous results [5]. Figures 6 (a) - (d) and 6 (e) - (h) show experimental impedance measurements performed on the liquid Pb electrode at different potentials along the reduction wave of Eu^{2+} and Sr^{2+}, respectively. Consequently, we concluded that the behaviors for Eu^{2+} and Sr^{2+} have similar tendencies.

Fig. 6. Impedance diagrams of $EuCl_2$ (a) –1.75 V, (b) –2.00 V, (c) –2.25 V, (d) –2.50 V (vs. Pt Q.R.E) and $SrCl_2$ (e) –1.50 V, (f) –1.75 V, (g) –2.00 V, (h) –2.25 V (vs. Pt Q.R.E) on the liquid Pb electrode for different applied potential values.

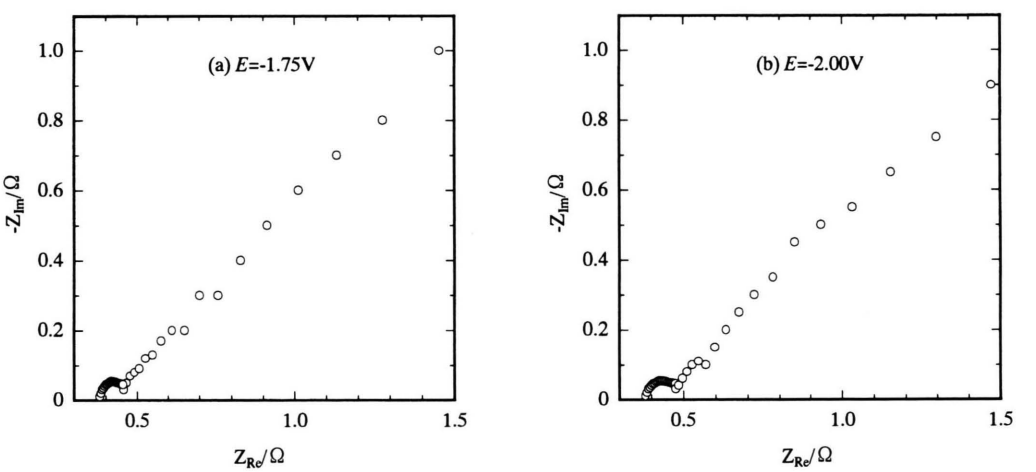

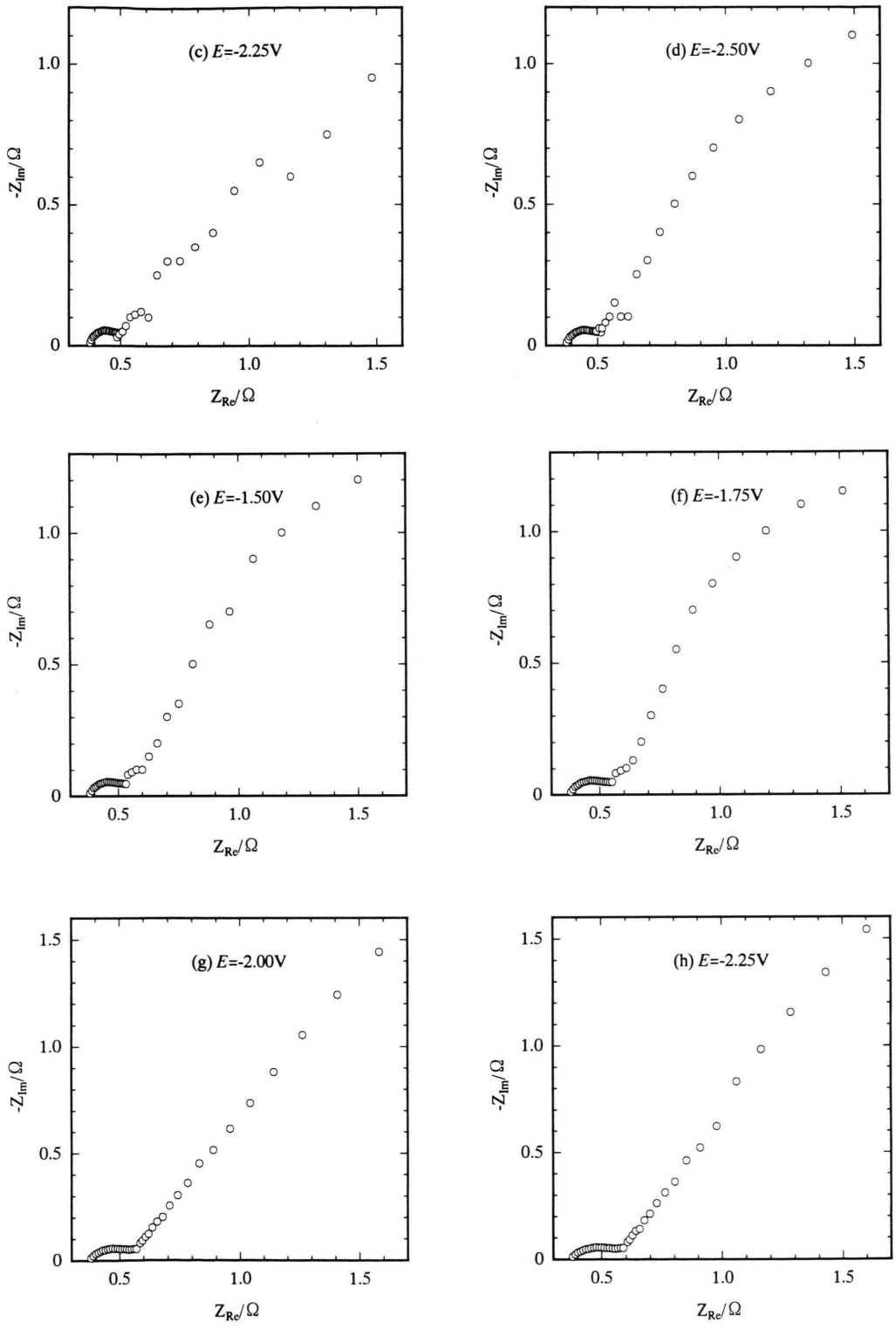

Fig. 6 (continued).

4. Conclusion

The impedance diagrams obtained are typical for a diffusion-convection controlled process at a tungsten electrode. The direct analysis of these diagrams verified that the Eu^{2+}/Eu and Sr^{2+}/Sr exchange is fast and involves two electrons: $Eu^{2+} + 2e^- + 3Pb \rightarrow EuPb_3$ and $Sr^{2+} + 2e^- + 3Pb \rightarrow SrPb_3$. The electrochemical reduction of Eu^{2+} and Sr^{2+} at the liquid Pb cathode is quasi-reversible. The diffusion coefficients of Eu^{2+} and Sr^{2+}, standard rate constants and diffusion layer thicknesses were determined.

[1] Y. I. Chang, L. C. Walters, J. E. Battles, D. R. Pederson, D. C. Wade, and M. J. Lineberry, ANL-IFR-125 (1990).
[2] Y. I. Chang et al., ANL-IFR-149 (1991).
[3] Y. I. Chang et al., ANL-IFR-246 (1994).
[4] W. J. Hamer, M. S. Malmberg, and B. Rubin, J. Electrochem. Soc. **112,** 750 (1965).
[5] M. Matsumiya, R. Takagi, and R. Fujita, J. Nucl. Sci. Technol. **34**, 310 (1997).
[6] M. Matsumiya, M. Takano, R. Takagi, and R. Fujita, Z. Naturforsch. **54a**, 739 (1999).
[7] M. Matsumiya, M. Takano, R. Takagi, and R. Fujita, J. Nucl. Sci. Technol. **35**, 836 (1998).
[8] M. Matsumiya, R. Takagi, and R. Fujita, J. Nucl. Sci. Technol. **35**, 137 (1998).
[9] P. Pasquier, D. Ferry, and G. Picard (in French), Electrochim. Acta **35**, 905 (1990).
[10] P. Pasquier and G. S. Picard, Electrochim. Acta **37**, 1149 (1992).
[11] R. Aogaki, K. Kitazawa, K. Fucki, and R. Mukaiko, Electrochim. Acta **23**, 867 (1978); ibid, **23**, 875 (1978).
[12] P. V. Polyakov, L. A. Isaeva, Yu. G. Mickhalev, and O. I. B. Ogdanovskii, Sov. Electrochem. **15**, 254 (1979).
[13] P. V. Polyakov, L. A. Isaeva, and Yu. G. Mickhalev, ibid. **16**, 952 (1980).
[14] M. Sluyters-Rehbach and J. H. Sluyters, Electroanalytical Chemistry, Vol. 4 (Edited by A. J. Bard), Marcel Dekker, Inc., New York 1970.
[15] A. V. Volkovich, Melts **7**, 106 (1994).
[16] R. D. Shannon, Acta Cryst. **A32**, 751 (1976).
[17] L. S. Kudin, G. G. Burdukovskaya, M. F. Butman, and K. S. Krasnov, Russ. J. Phys. Chem. **67**, 581 (1993).
[18] H. Matsuda and Y. Ayabe, Z. Electrochem. **59**, 494 (1955).